Wang, Di; Momo Takoudjou, Stéphane; Casella, Eric

LeWoS: A Universal Leaf-wood Classification Method to Facilitate the 3D Modelling of Large Tropical Trees Using Terrestrial LiDAR

# Methods in Ecology and Evolution

# LeWoS: A Universal Leaf-wood Classification Method to Facilitate the 3D Modelling of Large Tropical Trees Using Terrestrial LiDAR

**Di Wang[1]\*[†], Stéphane Momo Takoudjou[2,3][‡] and Eric Casella[4][§]**

*[1]Department of Built Environment, Aalto University, P.O. Box 14100, Aalto, 00076, Finland*
*[2]Institut de Recherche pour le Développement (IRD), URM AMAP, Montpellier cedex 5, France*
*[3]Plant Systematic and Ecology Laboratory, Higher Teacher's Training College, University of Yaoundé I, Yaoundé, Cameroon*
*[4]Centre for Sustainable Forestry and Climate Change, Forest Research, Farnham GU10 4LH, UK*

**Abstract**

1. Leaf-wood separation in terrestrial LiDAR data is a prerequisite for non-destructively estimating biophysical forest properties such as standing wood volumes and leaf area distributions. Current methods have not been extensively applied and tested on tropical trees. Moreover, their impacts on the accuracy of subsequent wood volume retrieval were rarely explored.

2. We present LeWoS, a new fully automatic tool to automate the separation of leaf and wood components, based only on geometric information at both the plot and individual tree scales. This data-driven method utilizes recursive point cloud segmentation and regularization procedures. Only one parameter is required, which makes our method easily and universally applicable to data from any LiDAR technology and forest type.

3. We conducted a two-fold evaluation of the LeWoS method on an extensive data set of 61 tropical trees. We first assessed the point-wise classification accuracy,

*Corresponding author.
[†]E-mail: di.wang@aalto.fi
[‡]E-mail: takoudjoumomo@gmail.com
[§]E-mail: eric.casella@forestresearch.gov.uk

yielding a score of $0.91 \pm 0.03$ in average. Secondly, we evaluated the impact of the proposed method on 3D tree models by cross-comparing estimates in wood volume and branch length with those based on manually separated wood points. This comparison showed similar results, with relative biases of less than 9% and 21% on volume and length, respectively.

4. LeWoS allows an automated processing chain for non-destructive tree volume and biomass estimation when coupled with 3D modelling methods. The average processing time on a laptop was 90s for 1 million points. We provide LeWoS as an open source tool with an end-user interface, together with a large data set of labelled 3D point clouds from contrasting forest structures. This study closes the gap for stand volume modelling in tropical forests where leaf and wood separation remain a crucial challenge.

**Keywords:** Terrestrial LiDAR, point cloud, tropical forest trees, component separation, segmentation, regularization, TreeQSM, volume

# 1 INTRODUCTION

Light Detection and Ranging (LiDAR) has revolutionized tree architecture measurements in past years (e.g., Dassot et al., 2011; Disney, 2019). Terrestrial Laser Scanning (TLS), or terrestrial LiDAR, is a ground-based scanning strategy that acquires three-dimensional (3D) coordinates in combination with radiometric information of objects by emitting laser pulses with wavelengths in the visible and near-infrared domain (Pfeifer et al., 2008). The acquired high-density point clouds allow very precise measurements of tree structures in a non-destructive way. These measurements include forest inventory (Liang et al., 2016), leaf angle distribution (Vicari et al., 2019b), structural parameters (Wang et al., 2016; Trochta et al., 2017), above-ground volume and biomass (AGB) (Calders et al., 2015; Momo Takoudjou et al., 2018; Gonzalez de Tanago et al., 2018). Moreover, allometric equations can be non-destructively performed with data derived from TLS (Momo Takoudjou et al., 2018; Lau et al., 2019).

However, several of these applications require prior knowledge of either leaf or woody components of trees. For example, understanding the radiation regime and photosynthetic processes relies on the quantification of the canopy leaf area and its spatial distribution.

Presence of wood may lead to a misinterpretation (Li et al., 2017). Accurate estimation of tree volume and AGB using Quantitative Structural Models (QSM, Raumonen et al., 2013) expects only woody structures. Presence of leaves is known to overestimate AGB (Calders et al., 2015). Moreover, opportunities for new applications such as mass and energy exchange, and net primary production partitioning of different components will emerge if leaf and wood can be separated in TLS data (Vicari et al., 2019a).

In the past decade, some efforts have been made to separate leaf and wood components in TLS point clouds (Béland et al., 2014; Hackenberg et al., 2015a; Ma et al., 2015; Hétroy-Wheeler et al., 2016; Wang et al., 2018; Vicari et al., 2019a). However, separating these components in TLS data still remains a main challenge, especially in ever-green tropical forests. Most of the available methods rely on laborious manual work or user inputs for specific data characteristics. These potential deficiencies hinder their applicability and universality for large data sets with diverse data qualities and field conditions (Vicari et al., 2019a).

Overall, existing methods were either based on geometric (Wang et al., 2018) or radiometric intensity features (Béland et al., 2014), or a combination of both (Zhu et al., 2018). Methods based on intensity usually have limited application scenarios. These methods are based on the assumption that leaf and wood components have different optical properties at the operating wavelength of the laser scanner (Tao et al., 2015). Nevertheless, such properties are generally influenced by the distance, a partial laser hit and its incidence angle (Kaasalainen et al., 2009). Intensity values have to be calibrated for each specific instrument (Calders et al., 2017), which limits the applicability of using intensity information for subsequent processing (Wang et al., 2018). Some research-led developments on multi-wavelength systems may help to differentiate leaf and wood in the future (Disney, 2019). In contrast, geometry based methods require only the 3D coordinates of points. Numerous geometry based methods use supervised machine learning, for which geometric features are learned for each point (Ma et al., 2015; Yun et al., 2016; Krishna Moorthy et al., 2019). These methods have shown promise and are potentially applicable to any point clouds (Disney et al., 2018). The drawback is that they require laborious and time consuming manual selection of training data. In addition, the distribution of training data greatly impacts the overall performance of machine learning methods (Wang et al., 2017). A combination of geometric and radiometric features may have advantage over using only one type (Zhu et al., 2018). Lastly, another preferable strategy is to deploy un-

supervised geometric methods that are free of training data (e.g., Hétroy-Wheeler et al., 2016). The critical point is to ensure robustness over different tree species, sensor configurations and data qualities (Vicari et al., 2019a). These unsupervised methods often look at specific geometric properties of components. Examples include presuming leaves being flat (Li et al., 2017), trunk and branch boundaries appear as circles or circle-like shapes (Tao et al., 2015), with linear structures across scales (Wang et al., 2018).

Previous methods were validated by assessing the point-wise separation (i.e., classification) accuracy. Their impacts of leaf and wood separation on subsequent TLS methods are still unknown (Vicari et al., 2019a). For quantitative ecology, tree volume or AGB is the key property of interest (Disney et al., 2018). Recent studies have shown that TLS, combined with QSM reconstruction methods, can be used to accurately estimate above-ground volume and AGB for large tropical trees (Momo Takoudjou et al., 2018; Gonzalez de Tanago et al., 2018). The accuracy of volume and AGB estimates depends on the quality of the reconstructed QSM, which in turn, relies on a well filtered point cloud of tree woody components. In general, tropical scenes are more challenging to reconstruct because of a poorer point cloud quality in the tree crown (Momo Takoudjou et al., 2018). Also, laborious and tedious manual removal of leaf points has to be carried out, which can require up to 15 hours per tree (Momo Takoudjou et al., 2018). An automated processing chain would greatly facilitate the usage of TLS for quantifying 3D structures of large tropical trees.

The objective of this study is to overcome these challenges. We first introduce a new generic unsupervised method for leaf-wood separation (hereafter LeWoS). The proposed method, which is based on recursive point cloud segmentation and a novel classification regularization routine, is fully automatic and highly versatile, as only one parameter is called. Then, its performance is evaluated on structurally varied and complex tropical trees in a two-fold fashion (Figure 1). Firstly, similar to previous studies, we assess the separation accuracies against manually delineated references. Second, we examine how sensitive to leaf-wood classification accuracy the subsequent QSM reconstruction is, by cross-comparing QSM reconstructions obtained from manually and automatically filtered point clouds. This cross-comparison gives a critical insight on how an automated process chain would impact downstream TLS ecology applications.
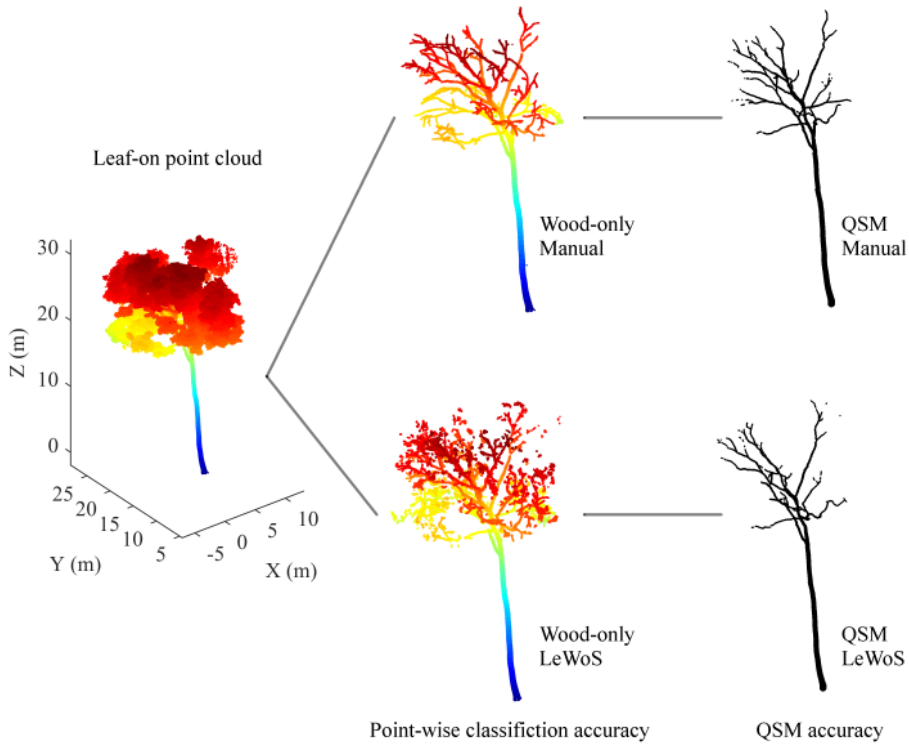
FIGURE 1: The two-fold evaluation strategy of this study.

## 2  MATERIALS AND METHODS

### 2.1  Study data

61 large tropical trees from the Eastern of Cameroon were included in this study. This set of trees was previously used for estimating large tropical tree biomass from TLS point clouds and calibrating allometric models (Momo Takoudjou et al., 2018; Momo et al., 2017). In total, the data set covered 15 different species. Tree height ranged from 8.7 to 53.6 m, with a mean value of $33.7 \pm 12.4$ m. Diameter at breast height (DBH) ranged from 10.8 to 186.6 cm, with a mean value of $58.4 \pm 41.3$ cm. See Table 2 in Momo Takoudjou et al. (2018) for a full description of the trees used in this study.

#### 2.1.1  TLS data

A time-of-flight scanner system Leica C10 Scanstation (Leica Geosystems, St. Gallen, Switzerland) was used for TLS data acquisitions. This scanner has a 360° horizontal and 270° vertical field-of-view, with an effective measurement rate up to 50,000 points per

second. A minimum of three scans were performed around each tree, with a sampling resolution of 0.0005 rad. Multi-scan data were later co-registered by the Leica Cyclone software (v. 9.1). The data size of the resulting individual tree point clouds ranged from 20,000 to 10,000,000 points.

### 2.1.2 Reference measurements

For each tree, leaf and wood points were manually separated using the Cyclone software (Figure 2). The required processing time was between 1 and 15 hr per tree (Momo Takoudjou et al., 2018). We also assigned to each wood point its respective branch order information derived from the QSM reconstructions (Lau et al., 2018). Specifically, each point was assigned to the branch order of its nearest cylinder in QSM.

In addition to leaf-wood references, destructive measurements of tree volumes and AGBs were carried out a few days after point cloud acquisitions. Although the aim of this study is not to validate the tree volume and AGB estimations from TLS, the destructive volume measurements have been also used to demonstrate the effectiveness of QSMs volume estimation based on an entirely automated processing chain, when compared with manual works.
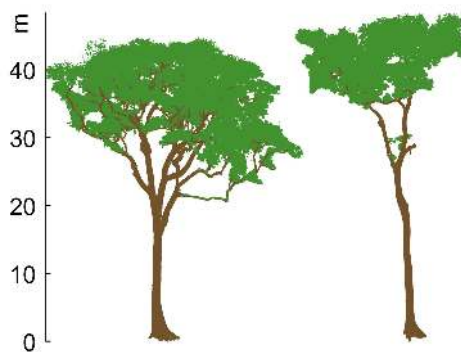


FIGURE 2: Examples of large tropical trees with manually separated leaf (green) and wood (brown) components.

## 2.2 LeWoS

Leaf-wood separation is inherently a binary classification problem, for which the goal is to assign either a wood or a leaf class label to each point. Our automated leaf-wood separation was motivated by the previous study of Wang et al. (2018), which evidenced that tree woody components can be identified as linear clusters after a robust point cloud

segmentation (i.e., semantic segmentation). The critical step is to establish an effective segmentation strategy that can adequately dispense points into clusters, so that each cluster contains either leaf or wood only points.

However, semantic segmentation of forest point clouds is a challenging task, as data quality is often diversified by scene complexity, laser scanner configurations, scanning campaign setups, point cloud co-registrations, and pre-processing filters. The proposed method in this study, LeWoS, tackles this challenge by three steps. Firstly, we adopt a graph based point cloud segmentation technique (e.g., Strom et al., 2010), and exercise it recursively in order to achieve a robust segmentation. Moreover, we alter direct wood extraction, which requires manual fine-tuning of some thresholds (Wang et al., 2018), to a class probability estimation. This transformation not only greatly increases the universality of the proposed LeWoS method, but also provides classification confidence information. Finally, we apply graph-structured class regularization (Landrieu et al., 2017) that operates on class probability to achieve a spatially smooth classification result.

The LeWoS algorithm was implemented in Matlab 2019a (The MathWorks, Inc., Natick, MA, USA).

### 2.2.1 Recursive segmentation

The proposed graph based point cloud segmentation method converts the conventional region growing method (Adams and Bischof, 1994) to a search of graph connected components problem. An undirected graph is represented as $G = (V, E)$, where $V = v_1, ..., v_n$ is a set of nodes. Each node $v_i \in V$ corresponds to a point in the point cloud, and the edges $e_{ij}$ in $E$ connect certain pairs of neighboring points.

We incorporate point cloud density and point-wise feature information in graph construction. Both properties were used by previous studies for leaf-wood separation as well (Vicari et al., 2019a). The exploited point-wise feature is *verticality* (i.e., the absolute value of the z-component of normal vector), which was previously verified as effective (Wang et al., 2018). We denote *verticality* as $N_z$, and $N_z \in [0, 1]$.

The normal vector of a point is estimated from the covariance matrix of its neighboring points. A covariance matrix measures the variation of each dimension from the mean with respect to each other. The normal vector at a point $p_i$ can be estimated as the eigenvector to the smallest eigenvalue of the covariance matrix given by:

$$\text{Cov}_{p_i} = \frac{\sum_{i=1}^{n} (p_i - \overline{p})(p_i - \overline{p})^T}{n},$$

(1)

where $\overline{p}$ is the barycenter of its $n$ neighboring neighbors.

Initially, a point $p_i$ is connected to its 10 nearest neighbors (Guinard and Landrieu, 2017), constructing a densely connected graph (Figure 3). Then, edges are further pruned according to the following conditions:

$$
e_{ij} = \begin{cases} \text{True} & \text{if} \begin{cases} \text{Condition 1} & |N_{zi} - N_{zj}| < N_z\_thres, \\ \text{Condition 2} & d_{ij} < \overline{d_{ij}} + \sigma_{d_{ij}}, \\ \text{Condition 3} & d_{ij} < \overline{\max(d_{ij})} + \sigma_{\max(d_{ij})}, \end{cases} \\ \text{False} & \text{otherwise,} \end{cases} \tag{2}
$$

where $N_z\_thres$ in Condition 1 is a threshold that controls feature similarity. A typical value is within the range of 0.1 to 0.2 (Wang et al., 2018). This is the only parameter that needs to be specified in the LeWoS algorithm. Its sensitivity analysis is given in section 3.2. $d_{ij}$ in Condition 2 refers to the Euclidean distance from a point to a neighboring point. $\overline{d_{ij}}$ stands for the mean distance to all its neighbors and $\sigma_{d_{ij}}$ is the standard deviation. Hence, Condition 2 controls local point cloud density connectivity. $\max(d_{ij})$ in Condition 3 stands for the farthest neighbor distance (i.e., effective range) of each point. Therefore, Condition 3 controls global point cloud density connectivity by removing very long edges.
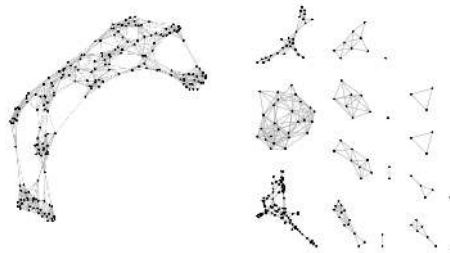


FIGURE 3: Example of graph construction. A node (black dot) is firstly connected to its 10 neighbors (left). The pruned graph is shown on the right. The connected components represent individual clusters.

The final pruned graph is a purposeful presentation in which only spatially adjacent points with similar features are connected (Figure 3). Then, segmentation of graph nodes (i.e., points) can be achieved by finding the connected components (Klasing et al., 2008). We apply this segmentation method recursively on each cluster resulted from previous segmentation. Point features and neighbors are updated after each iteration, so that leaf and wood points eventually become more distinguishable. The iteration stops when no

clusters can be further segmented. In practice, we limit the maximum iteration to 10, as the change becomes very minimal after then.

The $N_z$ feature used in this study is simple and effective. However, as shown in Figure 4b, it may result in coplanar clusters (Wang et al., 2018), in which several branches have similar *verticality* values. To improve the linearity feature saliency of branches, we further split branch clusters into individual branches using the method proposed in Raumonen et al. (2013) and Raumonen and Tarvainen (2018). This method uses small cover sets to grow surface and locate bifurcations. Consequently, the resulted clusters contain either leaf points or single branch points. We denote such a cluster as a segment (Figure 4c).
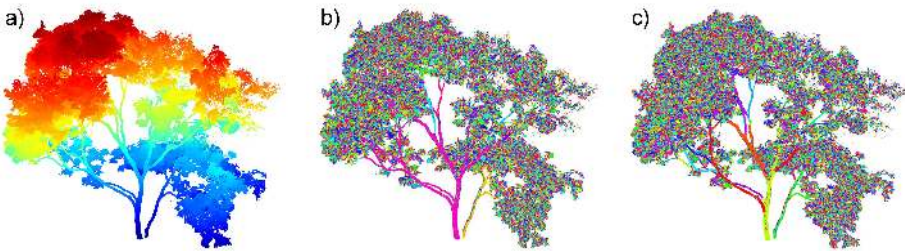


FIGURE 4: Example of segmentation steps. a) Original point cloud. b) Resulted segments from recursive graph segmentation. Each segment is randomly colored. c) Final segmentation result after branch splitting.

### 2.2.2 Class probability estimation

The woody components can be identified by examining the *Linearity* and *Size* of each segment generated from previous recursive segmentation step (Wang et al., 2018). Respectively, *Size* of a segment refers to the number of points in it, and *Linearity* is defined as $(\lambda_1 - \lambda_2)/\lambda_1$. $\lambda_1$, $\lambda_2$, and $\lambda_3$ are three eigenvalues from the covariance matrix (Equation 1), sorted in descending order. For segment level calculation, the covariance matrix is formed by all points in a segment, other than neighboring points.

Directly applying the above mentioned method implies two thresholds on the *Linearity* and *Size*. However, both thresholds need either user judgment or some test fine-tuning, which limits the algorithm's universality. Here, instead of directly extracting wood points by assigning hard thresholds (i.e., *hard labeling*), we infer a class probability by testing a range of possible threshold values, then count the frequency of a point being assigned as leaf or wood class (e.g., Raumonen and Tarvainen, 2018).

Specifically, the goal is to achieve a *soft labeling* set $S$ as:

$$\mathcal{S} = \left\{ pr \in [0,1]^{\mathcal{C}} \mid \sum_{k \in \mathcal{C}} pr_k = 1 \right\}, \tag{3}$$

so that the probability of each point $pr \in S$ being assigned to leaf and wood class $C \in$ $[leaf, wood]$ is determined. For a comprehensive examination, the threshold for *Linearity* was tested for values ranging from 0.70 to 0.94 with an increment of 0.02, and for values from 10 to 50 with an increment of 2 for the *Size* threshold. These ranges were chosen empirically to cover a set of plausible values. In total, 273 combinations were run. Each scenario determines the class a point belongs to, and so the frequency of a point being leaf or wood class. The relative frequency against all scenarios then provides the *soft labeling* set $S$ (Figure 5a).
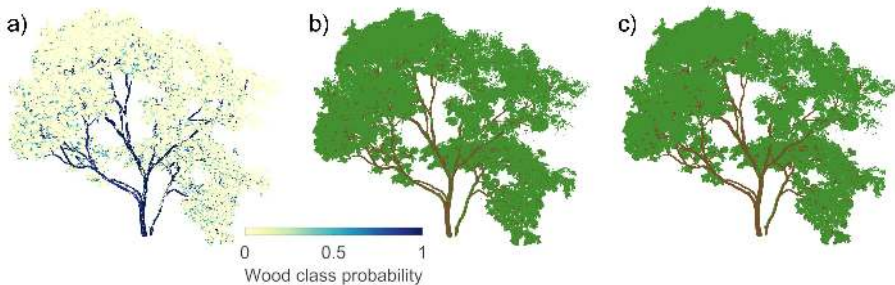


FIGURE 5: Example of class regularization. a) Point-wise wood class probability. Note that $pr_{leaf} = 1 - pr_{wood}$. b) Leaf-wood classification without regularization. c) Leaf-wood classification with regularization. Note that some misclassified stem and leaf points were corrected by regularization.

### 2.2.3 Class regularization

The *soft labeling* set $S$ indicates how confident we can assign a given class to a point. A direct classification would be labeling a point with the class that has largest probability. However, some branches may not be detected from previous steps for reasons such as heavy data occlusion and severe branch angulation. Consequently, their probabilities of being wood class are insignificant. The corresponding classification result then can be heterogeneous (Figure 5b), whereas a spatially smooth outcome is preferred.

A technique for solving such a problem is regularization (i.e., label smoothing) (Landrieu et al., 2017). The aim of class label regularization is to find an improved labeling set $S'$ with increased spatial smoothness while remaining as close as possible to the original

labeling set $S$. Expressly,

$$S^{'} = \underset{0 \in \Omega^{V}}{\arg\min}\{\Phi(S, S^{'}) + \gamma\Psi(S^{'})\}, \tag{4}$$

where $\Phi$ is the fidelity term that invokes the influence of the initial labeling set $S$. $\Psi$ is the regularizer that encourages solutions that are spatially smooth. $\gamma > 0$ is the regularization strength, and $\Omega$ stands for the search space.

We solve this minimization problem using the same strategy applied in Li et al. (2019), which was originally proposed in Landrieu et al. (2017). The fidelity term $\Phi$ is a linear one

$$\phi_{\text{linear}}(S, S^{'}) \doteq -\langle S, S^{'}\rangle = -\sum_{k \in \mathcal{C}} S_k S_k^{'}. \tag{5}$$

The regularizer $\Psi$ is structured by the adjacency graph $G = (V, E)$. The graph structured regularizer favors the fact that most adjacent nodes in the graph share the same label. Note that this graph slightly differs from the final graph in section 2.2.1. Here, it is not pruned by the feature similarity Condition 1 in Equation 2. The regularizer is factorized over the edges of $G$ (Geman and Reynolds, 1992) as:

$$\Psi(pr) \doteq \sum_{(i,j) \in E} \psi(pr_i - pr_j), \tag{6}$$

where $\psi(pr_i - pr_j)$ is the Potts model that returns 0 if two nodes share the same initial label, and 1 otherwise.

Finally, the objective function Equation 4 is solved by the $\alpha$-expansion algorithm (Boykov and Kolmogorov, 2004), which solves the multi-label energy-minimization problem iteratively. During each expansion operation, the problem is converted to a binary graph-cut problem that can be solved by the min-cut algorithm (Ding et al., 2001). The final classification resting on the improved labeling set $S^{'}$ is a spatially smoothed version where some misclassified points are corrected (Figure 5c).

## 2.3 Tree QSM

We respectively reconstruct the woody components of trees generated from manual delineation (hereafter QSM_TLS_Manual) and automatic detection by LeWoS (hereafter QSM_TLS_Auto), using the QSM method developed in Raumonen et al. (2013) (Figure 1). This method was successfully used in previous studies for generating 3D tree models and estimating AGBs (Calders et al., 2015; Raumonen et al., 2015; Gonzalez de Tanago

et al., 2018). The method firstly slices wood points of a single tree into separate segments to deduce the tree topological branching architecture. Then, these segments are fitted by a series of cylinders. The resulting cylinder model (i.e., QSM) is a collection of cylinders embedded with branching topological clue, from which the volume and length of different branch orders can be calculated.

We used the latest development (v. 2.3) of the QSM algorithm retrieved from Åkerblom (2017). The method is sensitive to a particular input parameter *PatchDiam* (i.e., surface patches diameter) that needs to be optimized on specific data (Gonzalez de Tanago et al., 2018; Lau et al., 2018). Moreover, 10 QSM models for each tree are produced due to the randomness involved in the processing steps of this method (Calders et al., 2015). We then report the mean and standard deviation from these 10 models. A detailed explanation of the QSM method and its parameters can be found in Raumonen et al. (2013), Raumonen et al. (2015), Calders et al. (2015), Newnham et al. (2015), and Lau et al. (2018).

## 2.4 Assessment

We evaluate the effectiveness of LeWoS on 3D tree models (or scenes) from two parts.

First, point-wise classification accuracy was reported. This metric measures the capability of the LeWoS method for differentiating leaf and wood components in a tree point cloud. The overall accuracy is evaluated as:

$$\text{Accuracy} = \frac{\text{TP} + \text{TN}}{\text{TP} + \text{TN} + \text{FP} + \text{FN}}, \tag{7}$$

where TP represents true positive (i.e., wood), and TN the true negative (i.e., leaf). FP and FN stand for false positive (type I error) and false negative (type II error), respectively. In addition, we reported results from the model sensitivity and specificity. Sensitivity measures the true positive rate which is the ratio of correctly classified wood points. Specificity gives the true negative rate, thus it measures the correct rate for leaf points, given by:

$$\text{Sensitivity} = \frac{\text{TP}}{\text{TP} + \text{FN}}, \tag{8}$$

$$\text{Specificity} = \frac{\text{TN}}{\text{TN} + \text{FP}}. \tag{9}$$

Second, we cross-compared the tree volume and branch length estimations between QSM_TLS_Manual and QSM_TLS_Auto. Branches with diameter less than 5 cm were

excluded from the analysis to be consistent with the study of Momo Takoudjou et al. (2018). For individual comparisons, the bias (i.e., unsigned residual), and its relative value were reported. The mean absolute deviation (MAD) and mean absolute percentage deviation (MAPD) were calculated for group comparisons as:

$$\text{Bias} = |\text{QSM\_TLS\_Manual} - \text{QSM\_TLS\_Auto}|, \tag{10}$$

$$\text{Bias}(\%) = 100\% \times \left| \frac{\text{QSM\_TLS\_Manual} - \text{QSM\_TLS\_Auto}}{\text{QSM\_TLS\_Manual}} \right|, \tag{11}$$

$$\text{MAD} = \frac{1}{n} \sum_{t=1}^{n} |\text{QSM\_TLS\_Manual}_t - \text{QSM\_TLS\_Auto}_t|, \tag{12}$$

$$\text{MAPD} = \frac{100\%}{n} \sum_{t=1}^{n} \left| \frac{\text{QSM\_TLS\_Manual}_t - \text{QSM\_TLS\_Auto}_t}{\text{QSM\_TLS\_Manual}_t} \right|. \tag{13}$$

## 3   RESULTS

The results of this study are divided into four parts: 1) Sensitivity analysis of the *Patch-Diam* parameter in QSM; 2) Sensitivity analysis of the $N_z\_thres$ parameter in LeWoS; 3) Evaluation of point-wise classification of all trees; 4) Assessment of the impacts of automated leaf-wood separation on QSM volume and length estimations at both the whole single tree and branch levels.

### 3.1   Sensitivity analysis of QSM parameter

We used 10 randomly selected trees to infer an optimal value of *PatchDiam*. QSMs were constructed over manually delineated wood points of these selected trees. The derived QSM above ground volumes were compared to the destructive reference measurements. A minimum error was reached for *PatchDiam* of 3 cm (Table 1). This is in agreement with the reported results in previous studies (Calders et al., 2015; Newnham et al., 2015; Gonzalez de Tanago et al., 2018). Therefore, 3 cm *PatchDiam* was selected for QSM constructions over both manually delineated and automatically detected woody components of all trees.

### 3.2   Sensitivity analysis of LeWoS parameter

We conducted a two-fold sensitivity analysis of the $N_z\_thres$ parameter in LeWoS. Accuracy on both point-wise classification and QSM volume estimation were examined (Table

TABLE 1
QSM *PatchDiam* sensitivity analysis on volume estimation.

| PatchDiam | MAD (m³) | MAPD (%) |
|-----------|----------|----------|
| 0.01 | 1.22 | 13.98 |
| 0.02 | 0.90 | 11.65 |
| 0.03 | 0.67 | 9.96 |
| 0.04 | 0.76 | 11.22 |
| 0.05 | 0.75 | 11.75 |
| 0.06 | 0.88 | 12.71 |

*PatchDiam*, surface patches diameter; QSM, quantitative structure models; MAD, mean absolute error; MAPD, mean absolute percentage error.

2). For point-wise classification, a $N_z\_thres$ of 0.125 and 0.15 gave the comparable highest overall accuracy, while 0.1 showed marginally worse results. However, QSM volume estimation indicated a clear optimal performance with $N_z\_thres$ being 0.15. Therefore, 0.15 $N_z\_thres$ was selected for all trees in this study.

TABLE 2
$N_z\_thres$ sensitivity analysis.

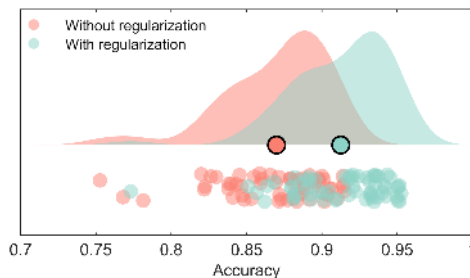| $N_z\_thres$ | Point-wise classification accuracy | QSM volume MAD (m³) |
|--------------|-----------------------------------|---------------------|
| 0.075 | 0.877 | 2.56 |
| 0.1 | 0.906 | 1.85 |
| 0.125 | 0.915 | 1.12 |
| 0.15 | 0.913 | 0.80 |
| 0.175 | 0.899 | 1.14 |
| 0.2 | 0.887 | 0.97 |
| 0.215 | 0.878 | 1.29 |

### 3.3 Point-wise classification



FIGURE 6: Raincloud plot (Allen et al., 2019) showing the distribution of classification accuracies of all trees. Black circles indicate mean values.

For 61 large tropical trees, the LeWoS method showed an overall classification accu-
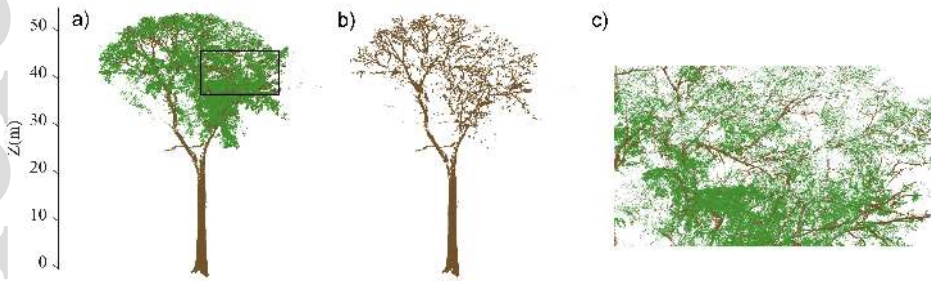
FIGURE 7: Example of point-wise classification result on a large tree. a) Overall classification result. b) Extracted wood points. c) Magnified view corresponds to the black rectangle area in a).

racy of $0.91 \pm 0.03$, with a sensitivity of $0.92 \pm 0.04$ and a specificity of $0.89 \pm 0.06$. The rather balanced sensitivity and specificity indicated that our method had equal effectiveness on detecting either leaf or wood points. Most trees had an accuracy between 0.90 and 0.95 (Figure 6), while the most frequent accuracy was approximately 0.94. A visual example of the outcome of this classification is reported in Figure 7.

Branch level classification assessment is impractical because of lacking leaf references at the individual branch level. Instead, we evaluated the integrity (i.e., percentage of number of detected points over reference points) of wood points detection at different branch orders (Table 3). Overall, the integrity decreased with increasing branch orders. For tree stems, on average 92.8% points were successfully detected. Approximately 75% points of the first order branches were kept. However, the integrity decreased rather quickly for children branches. For example, only slightly more than half points were detected for the 4th order branches, whereas undetected points were incorrectly classified as leaves.

TABLE 3
Results on different branch orders.

| Branch order | Point-wise classification | | Volume | | | Length | | |
|---|---|---|---|---|---|---|---|---|
| Branch order | Ratio (%) | Integrity (%) | Ratio (%) | MAD ($m^3$) | MAPD (%) | Ratio (%) | MAD (m) | MAPD (%) |
| 0 | 71.65 | 92.82 | 85.88 | 0.65 | 8.31 | 40.56 | 2.70 | 7.51 |
| 1 | 12.23 | 75.17 | 9.82 | 0.26 | 55.94 | 28.72 | 8.77 | 36.63 |
| 2 | 9.39 | 67.00 | 3.57 | 0.17 | 210.79 | 20.59 | 15.07 | 151.77 |
| 3 | 4.72 | 60.69 | 1.40 | 0.10 | 124.23 | 12.20 | 15.00 | 107.20 |
| 4 | 1.96 | 52.54 | 0.41 | 0.06 | 152.39 | 4.77 | 12.81 | 140.78 |
| 5 | 0.67 | 47.89 | 0.12 | 0.02 | 224.93 | 1.56 | 6.88 | 236.24 |

Order 0 refers to tree stems. Ratio, proprtion to the
whole tree. i.e., the sum over the orders $\simeq 100$.

## 3.4 QSM modelling

To assess the accuracy on QSM modelling, we cross-compared the volume and length estimates between QSM_TLS_Manual and QSM_TLS_Auto. The assessment was done at the entire tree level and at the level of individual branch orders. For an independent evaluation of the effectiveness of coupling automatic wood extraction with QSM, we also inspected the accuracies of volume estimations by QSM_TLS_Auto, against the reference volumes from destructive measurements.

### 3.4.1 Tree level

Compared to destructive volume measurements, the QSM_TLS_Auto showed a MAD of 4.35 $m^3$ with a MAPD of $20.2 \pm 19.1\%$ (Figure 8a). The $R^2$ of the linear regression line (Figure 8a black line) was 0.91. The slope was 0.55, which indicates that the QSMs significantly underestimated the tree volumes, especially for very large trees due to strong occlusion levels. As a benchmark, the QSM_TLS_Manual performed similarly, showing a MAD of 3.86 $m^3$ with a MAPD of $16.7 \pm 17.2\%$ (Figure 8b). The slope was 0.57 with a $R^2$ of 0.91. Both tests showed optimal results for those trees with volumes less than 20 $m^3$ (DBH < ~90 cm), but had large biases for larger trees.

For cross-comparisons, QSM_TLS_Manual and QSM_TLS_Auto conferred high agreements for both the total volume (Figure 8c) and the branch length estimations (Figure 8d). The agreement on volume estimation showed a $R^2$ of 0.99 and a slope of 0.95 for the linear regression line (Figure 8c orange line), with a MAD of 0.79 $m^3$, leading to a MAPD of $8.9 \pm 11.1\%$. The $R^2$ of the linear regression for branch length estimations (Figure 8d orange line) was 0.89 with a line slope of 0.99. The MAD was 39.64 m with a MAPD of $20.9 \pm 14.3\%$. The fitted linear regression lines (Figure 8c and d) both showed modest underestimates. The analysis of the residuals did not reveal any systematic biases (Figure 9). However, the disparities and uncertainties were more preponderant for larger trees (volume > 20 $m^3$). Overall, the QSM_TLS_Auto underestimated the volume and branch length by 5.0% and 19.2%, respectively.

### 3.4.2 Branch level

We further cross-compared the volume and branch length estimates by QSM_TLS_Manual and QSM_TLS_Auto on different branch orders. The MAD was smallest for tree stems, with a volume MAPD of 8.3% and a length MAPD of 7.5%, respectively (Table 3). The
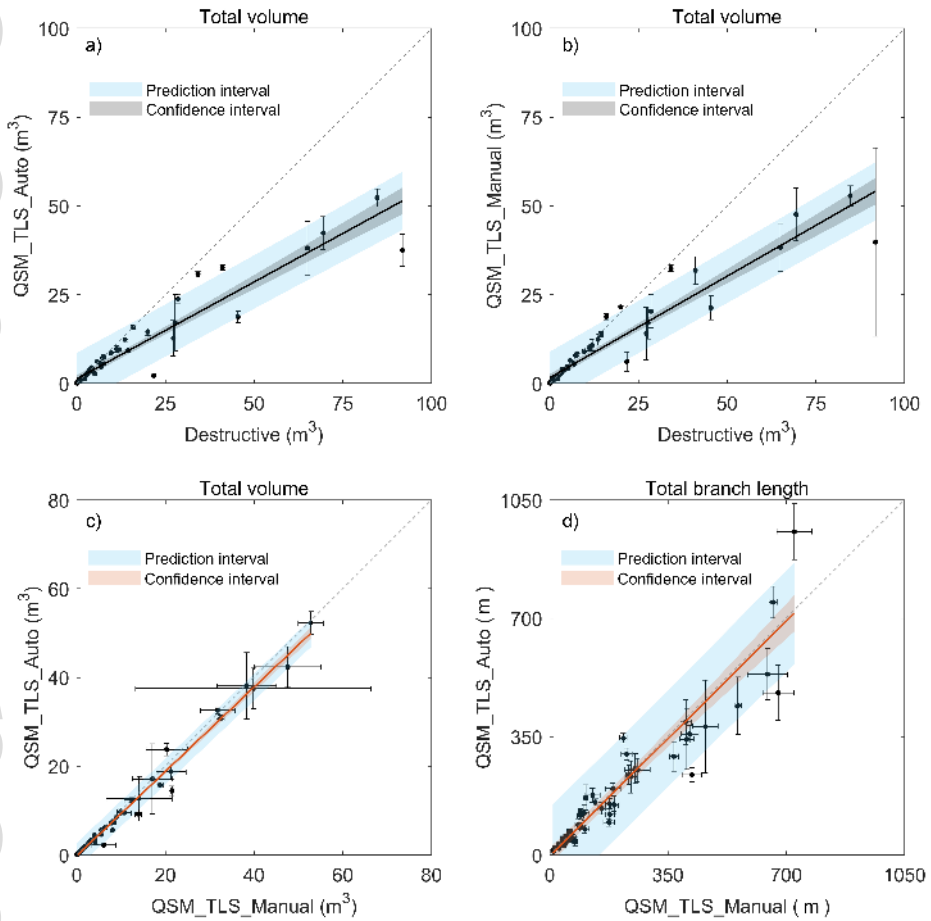
FIGURE 8: Comparisons of total volume and branch length estimations. a) QSM_TLS_Auto volumes against destructive volume measurements. b) QSM_TLS_Manual volumes against destructive measurements. c) QSM_TLS_Manual volumes against QSM_TLS_Auto volumes. d) QSM_TLS_Manual branch lengths against QSM_TLS_Auto branch lengths.

biases increased drastically with increases in branch order. For example, the MAPDs exceeded 100% already since the second branch order, indicating an inconsistent topology between QSM_TLS_Manual and QSM_TLS_Auto.

This inconsistency was not observed when analyzing the disparities on different branch diameter groups extracted from the individual reconstructed cylinders in QSMs. In Table 4, cylinders in the reconstructed QSMs of all 61 trees were grouped into seven diameter classes. The volume and branch length biases were rather consistent, but largest cylinder segments showed the smallest relative biases. This indicates that QSM_TLS_Manual and QSM_TLS_Auto were compatible with each other on the
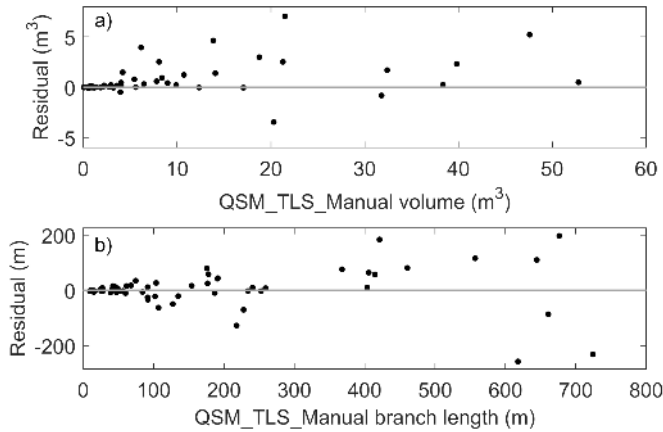
FIGURE 9: Analysis of a) volume and b) branch length estimation residuals.

reconstructed tree geometry, but had inconsistent tree topology.

TABLE 4
Volume and length bias on different diameter groups.

| Diameter group (cm) | Number of cylinder | Volume bias (%) | Length bias (%) |
|---|---|---|---|
| 5 - 15 | 1167 | 15.57 | 3.25 |
| 15 - 25 | 647 | 37.50 | 27.77 |
| 25 - 35 | 141 | 29.43 | 23.82 |
| 35 - 45 | 96 | 22.66 | 20.99 |
| 45 - 55 | 29 | 37.16 | 6.74 |
| 55 - 65 | 5 | 13.94 | 14.34 |
| > 65 | 6 | 11.50 | 2.70 |

Include tree stems.

## 3.5 Algorithm implementation and efficiency

The LeWoS algorithm developed here was implemented as an open source Matlab package with an end-user interface. We also provided a standalone version that does not require a Matlab to be installed on the user's machine. The tool is easy to use. Tests showed that it can process $\sim$1 million points within 90 seconds on a laptop, and has a linear relationship with the total number of points (Figure 10). The laptop we used to run the algorithm has the following specifications: Windows 10, Intel® Core™ i7-8850H and 32 GB RAM.
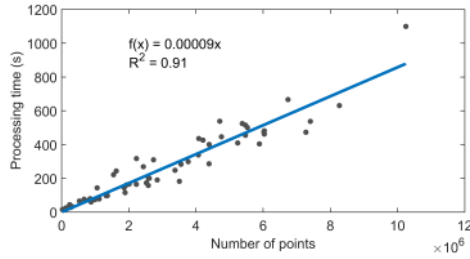
FIGURE 10: The relationship between the runtime of LeWoS with point cloud size.

# 4  DISCUSSION

We proposed a new, highly versatile and robust tool for leaf-wood separation from TLS point clouds. We evaluated the effectiveness of the LeWoS method on two aspects: (a) assessing the point-wise separation accuracy using an extensive data set with manual leaf-wood labelling and, (b) evaluating the impacts of automated leaf-wood separation on tree QSM modelling. The examination of (b) put a new perspective on completing an automated processing chain for 3D tree modelling using TLS, especially for large data sets.

## 4.1  Accurate point-wise classification

We tested the LeWoS algorithm on 61 large leaf-on tropical trees. These trees were tall, and had very large crown sizes and complexities. These factors led to an extreme challenging condition for acquiring high quality TLS data, especially due to heavy occlusions. Jointly, this further introduced large uncertainties in the 3D tree reconstructions (Gonzalez de Tanago et al., 2018).

The method proposed here achieved similar separation results compared to previous studies on less challenging data sets. For example, Ma et al. (2015) used a supervised gaussian mixture model (GMM) to separate photosynthetic and non-photosynthetic components from TLS data. Their overall accuracy for single tree data was 82.6%, and further improved to 99.6% after applying a series of post filters. Yun et al. (2016) used a support vector machine (SVM) model for four single trees, and the achieved overall accuracy was from 89.1% to 93.5%. Zhu et al. (2018) deployed a random forest classifier using both radiometric and geometric features. Their testes on 10 plots showed an overall accuracy of 0.84. Zhou et al. (2019) similarly used the random forest classifier to separate leaf and wood points of nine trees, with an accuracy of 0.93. Wang et al. (2018) developed an

unsupervised segmentation method and obtained 0.88 average accuracy on several plot-level data sets. Vicari et al. (2019a) achieved average 0.89 accuracy for 10 temperate and tropical trees. Both Wang et al. (2018) and Vicari et al. (2019a) share the same advantage with our method of being fully automatic.

The LeWoS method inventively converted the direct wood segmentation to a class probability estimation. This further enabled us to deploy a class regularization technique. Results showed that this regularization significantly improved separation accuracies (Figure 6). Different from previous studies (Vicari et al., 2019a; Ma et al., 2015) who used several post-processing filters to improve the accuracy, our class regularization technique is an embedded global optimization routine that does not need the design of local filters for specific data sets.

Visual inspection revealed that the separation difficulty occurred mainly inside tree crowns, whereas tree stems were generally well detected (e.g., Figure 7 and Table 3). Tree crowns often have poor data qualities with significant level of occlusions. Some branches were fragmented in point clouds (Figure 7c), which prevented them from being identified, as our method detects linear structures. As suggested by Vicari et al. (2019a), data quality poses one of the main prerequisites for successful leaf-wood separation. This challenge is even more severe for tropical forests (Gonzalez de Tanago et al., 2018). Data quality depends on multiple factors such as laser scanners characteristics, scanning setups, co-registration accuracy, and occlusion levels. To overcome these challenges, Vicari et al. (2019a) suggested using high TLS resolution levels and optimal field scanning protocols, and co-registration methodologies such as used by Wilkes et al. (2017). Another strategy is to apply on-the-fly adjustment (Paynter et al., 2018) for TLS data quality control.

One tree in this study had much worse classification accuracy (i.e., 0.77) than others (Figure 6) and was further diagnosed (Figure 11). The tree species was *Pycnanthus angolensis*, and was one of the smallest trees of this study displaying a DBH of 14 cm. The poor classification accuracy comes from the fact that many leaf points were identified as wood. The LeWoS method detected linear structures by assuming that tree woody components appear to be linear across various scales, while leaves are generally flat or scattered (Wang et al., 2018). However, under some circumstances, single leaves or a cluster of leaves may appear to be linear as well. Consequently, these leaves were identified as wood. A potential solution is to lower the $N_z\_thres$ threshold to avoid false segments. For example, by lowering the threshold to 0.05, the *Pycnanthus angolensis*

tree was successfully processed (Figure 11).

The intention on detecting tree linear structures may impede the applicability of the proposed method for coniferous trees, where individual needle appears to be linear as well. However, in practice, individual needles are improbably resolved in any tree or plot level LiDAR point clouds, due to its small size and the dense clumped foliage of conifer trees (Du et al., 2019). Usually, the recognition of needles and branches in the point cloud is even visually very difficult (Pfeifer et al., 2004). Therefore, less attention was paid on needle level studies using TLS. Nevertheless, the method in this study is able to detect the stems and some large branches of conifer trees, if they are resolved in the TLS point clouds (see Supporting Information).



FIGURE 11: Left to right: manual reference, classification result with $N_z\_thres$ being 0.15 (i.e., the value used in this study), 0.10, and 0.05.

## 4.2   Impacts of leaf-wood separation on tree 3D modelling

Previous studies on leaf-wood separation evaluated their methodologies for point-wise classification accuracy only (e.g., Ma et al., 2015; Wang et al., 2018; Vicari et al., 2019a). The impacts of leaf-wood separation on 3D tree modelling remained largely unexplored, except Vicari (2019).

QSM is by far the most popular method for reconstructing the 3D woody structure of trees. Two recent studies applied QSM for estimating the volume and AGB of large tropical trees (Momo Takoudjou et al., 2018; Gonzalez de Tanago et al., 2018). Although different QSM algorithms were used, both studies showed large biases for larger trees (defined as DBH > 90 cm in Momo Takoudjou et al. (2018) and DBH > 70 cm in Gonzalez de Tanago et al. (2018)). Manual correction was necessary in Momo Takoudjou

et al. (2018) to improve the quality of QSMs. Our tests showed similar results, even when using manually delineated wood points (Figure 8b). A potential reason is attributed to the buttress in large trees (Markku et al., 2015; Gonzalez de Tanago et al., 2018), whereas only cylinder fitting was used in this study. Disney et al. (2018) compared the volumes of buttressed trunks estimated using a closed triangulation surface model with those estimated from cylinder fitting, and found that the volume differences could be as high as 45%. We note that it is possible to model buttress with such mesh models in the QSM tool by Raumonen et al. (2013).

Nevertheless, this study demonstrated that QSMs on top of automatically detected wood points had similar total volume (Figure 8c) and branch length (Figure 8d) estimates, when compared with QSMs based on manually delineated wood points. The volume MAPD was less than 9%, and length MAPD was larger at ∼21%. Volumes, however, mostly rest in tree stems for large tropical trees. For example, stems represented 85.9% (Table 3) volumes in this study, but only 40.6% lengths. Stems, together with the first and second order branches, shared more than 99% volumes in this study. This indicates that the effectiveness of total volume estimation depends mainly on how well the dominant coarse branches are detected and modeled. LeWoS showed high detection rates for coarse branches, thus is capable of producing reliable volume estimates, when coupled with QSM methods. Furthermore, the relative biases between QSM on automatically detected wood points and QSM on manual wood points, are with the same magnitude of the uncertainty introduced by QSM itself. For example, the reported mean of unsigned relative error (i.e. MAPD) for volume estimation in Momo Takoudjou et al. (2018) was 12% on the same data set. The relative error of branch length estimation from QSM was reported as 20% (Lau et al., 2018). We therefore consider that our method can be positively combined with QSM methods for an automatic quantification of tree total volume, AGB (with wood density), and branch lengths.

On the other hand, this study also suggested that the tree topology did not match between QSMs on automatically detected wood points and QSMs on manual wood points. The inconsistency could be originated from incorrect leaf-wood separation inside tree crowns, but also from the randomness involved in QSM reconstruction (Raumonen et al., 2013). For example, the analysis on the volume and length bias on different diameter groups (Table 4) did not reveal the same disparity magnitude as on branch orders (Table 3), indicating that most branches were successfully reconstructed but were assigned

to different orders. A recent study by Lau et al. (2018) examined detailed tropical tree architecture based on QSM. Manual branch-by-branch pairing had to be performed, implying that the topology regenerated automatically by QSM is unreliable, and involves a certain degree of randomness. They also revealed that QSM reconstructed less than 56% of thin branches (diameter between 10 and 30 cm). In fact, accurate reconstruction of thin branches is a known problem of QSM itself (Kaasalainen et al., 2014; Hackenberg et al., 2015b). Moreover, branching order is a very sensitive parameter, and can be easily influenced if a point cloud is not properly filtered (Lau et al., 2018). We therefore argue that the inconsistent topology between QSMs on automatically detected wood points and QSMs on manual wood points does not imply that automated leaf-wood separation is not able to correctly reconstruct the tree architecture. A separate study similar to Lau et al. (2018) should be carried out to further clarify it.

## 4.3 LeWoS

The presented leaf-wood separation algorithm, LeWoS, is fully automatic and highly versatile. Previous unsupervised methods require the optimization of a set of parameters (Wang et al., 2018; Vicari et al., 2019a). The fact that the proposed LeWoS method only requires one parameter makes it very generalizable. For leaf-wood separation, we also showed that this only parameter is rather insensitive (Table 2 and Supporting Information). However, further tests should also give insight into how this parameter is related to different data sources and tree species.

The hardcore of our method is the robust recursive graph-based segmentation. The local density connectivity control is totally data-driven, and can be applied to any point clouds. The feature connectivity control can be further enriched by replacing the *verticality* with more sophisticated features, or gathering more features. For example, combining radiometric features from new hyper-spectral LiDAR sensor systems (Chen et al., 2019) may help to solve the problem reported in Figure 11.

Although we tested the LeWoS method on individual tropical trees in this study (currently QSM only works for single trees), this leaf-wood separation method is fully applicable to plot-wide data and different forest types. Backroom tests on other tropical, temperate, and boreal forests have shown equal effectiveness of our method for extracting tree woody components (see Supporting Information). In addition, the LeWoS method has a great potential in facilitating the plot-wide single tree segmentation (see Supporting

Information).

LeWoS was developed and distributed as an open-source Matlab tool with an end-user interface (see Supporting Information). We also provide a standalone executable. The tool is easy to install and work with. We hereon provide the community an alternative tool and hope it can facilitate the usage of TLS for forest ecological applications.

# 5   CONCLUSIONS

In this study, we presented a fully automatic and highly versatile approach named LeWoS to separate tree leaf-wood components from LiDAR point clouds. This method is data-driven and dispenses with manual delineation of training data. It is also free from restricted assumptions of tree architecture and data sources. Furthermore, we demonstrated that our method can be coupled with QSM methods to frame an automatic processing chain for tree structural quantification using TLS.

We tested this method on 61 large tropical trees. The achieved point-wise separation accuracies were similar to other reported results in the literature, with a mean value of $0.91 \pm 0.03$. For the first time, we also demonstrated the impacts of automated leaf-wood separation on 3D tree QSM modelling. Results showed that QSM tree volume and branch length estimations using automatically detected wood points were similar to those based on manual delineation of point clouds. Our work highlights the potential of combining automated leaf-wood separation with QSM reconstructions for accurate and automatic tree volume estimation.

The LeWoS method provides a significant advance in TLS ecology studies. The implemented algorithm is multi-threaded, and can process large point clouds in a rapid and consistent way. We hope this open-source tool can be used in the future by the TLS ecology community to automate certain processing chains.

# ACKNOWLEDGEMENTS

TF010038 from the Global Environment Facility). We are grateful to the AMAP French Lab for sharing TLS data. We thank AMAP members Nicolas Barbier, Grégoire Vincent, and Olivier Martin-Ducup for their discussions and comments on an earlier draft of this study.

## AUTHORS' CONTRIBUTIONS

D.W. and E.C. conceived the ideas; D.W. designed methodology and analyzed the data; S.M.T. collected the data; D.W. led the writing of the manuscript. All authors contributed critically to the drafts and gave final approval for publication.

## DATA ACCESSIBILITY

The source code and standalone executable for LeWoS are available at github.com/dwang520/LeWoS and archived at https://doi.org/10.5281/zenodo.3516856. The TLS data and destructive references of tropical trees are owned by the AMAP French lab, through the original publication Momo Takoudjou et al. (2018). The data sets are free to download at the Dryad Digital Repository https://doi.org/10.5061/dryad.10hq7. The manually labelled point clouds are additionally available at https://doi.org/10.5061/dryad.np5hqbzp6. For questions on data sets, please contact: takoudjoumomo@gmail.com.

## References

Rolf Adams and Leanne Bischof. Seeded region growing. *IEEE Transactions on pattern analysis and machine intelligence*, 16(6):641–647, 1994.

Micah Allen, Davide Poggiali, Kirstie Whitaker, Tom Rhys Marshall, and Rogier A Kievit. Raincloud plots: a multi-platform tool for robust data visualization. *Wellcome open research*, 4, 2019.

Martin Béland, Dennis D Baldocchi, Jean-Luc Widlowski, Richard A Fournier, and Michel M Verstraete. On seeing the wood from the leaves and the role of voxel size in determining leaf area distribution of forests with terrestrial lidar. *Agricultural and Forest Meteorology*, 184:82–97, 2014.

Yuri Boykov and Vladimir Kolmogorov. An experimental comparison of min-cut/max-flow algorithms for energy minimization in vision. *IEEE Transactions on Pattern Analysis & Machine Intelligence*, (9):1124–1137, 2004.

Kim Calders, Glenn Newnham, Andrew Burt, Simon Murphy, Pasi Raumonen, Martin Herold, Darius Culvenor, Valerio Avitabile, Mathias Disney, John Armston, et al. Non-destructive estimates of above-ground biomass using terrestrial laser scanning. *Methods in Ecology and Evolution*, 6(2):198–208, 2015.

Kim Calders, Mathias I Disney, John Armston, Andrew Burt, Benjamin Brede, Niall Origo, Jasmine Muir, and Joanne Nightingale. Evaluation of the range accuracy and the radiometric calibration of multiple terrestrial laser scanning instruments for data interoperability. *IEEE Transactions on Geoscience and Remote Sensing*, 55(5):2716–2724, 2017.

Biwu Chen, Shuo Shi, Jia Sun, Wei Gong, Jian Yang, Lin Du, Kuanghui Guo, Binhui Wang, and Bowen Chen. Hyperspectral lidar point cloud segmentation based on geometric and spectral information. *Optics Express*, 27(17):24043–24059, 2019.

Mathieu Dassot, Thiéry Constant, and Meriem Fournier. The use of terrestrial lidar technology in forest science: application fields, benefits and challenges. *Annals of forest science*, 68(5):959–974, 2011.

Chris HQ Ding, Xiaofeng He, Hongyuan Zha, Ming Gu, and Horst D Simon. A min-max cut algorithm for graph partitioning and data clustering. In *Proceedings 2001 IEEE International Conference on Data Mining*, pages 107–114. IEEE, 2001.

Mathias Disney. Terrestrial lidar: a three-dimensional revolution in how we look at trees. *New Phytologist*, 222(4):1736–1741, 2019.

Mathias I Disney, Matheus Boni Vicari, Andrew Burt, Kim Calders, Simon L Lewis, Pasi Raumonen, and Phil Wilkes. Weighing trees with lasers: advances, challenges and opportunities. *Interface Focus*, 8(2):20170048, 2018.

Shenglan Du, Roderik Lindenbergh, Hugo Ledoux, Jantien Stoter, and Liangliang Nan. Adtree: Accurate, detailed, and automatic modelling of laser-scanned trees. *Remote Sensing*, 11(18), 2019. ISSN 2072-4292.

Donald Geman and George Reynolds. Constrained restoration and the recovery of discontinuities. *IEEE Transactions on Pattern Analysis & Machine Intelligence*, (3):367–383, 1992.

Jose Gonzalez de Tanago, Alvaro Lau, Harm Bartholomeus, Martin Herold, Valerio Avitabile, Pasi Raumonen, Christopher Martius, Rosa C Goodman, Mathias Disney, Solichin Manuri, et al. Estimation of above-ground biomass of large tropical trees with terrestrial lidar. *Methods in Ecology and Evolution*, 9(2):223–234, 2018.

S. Guinard and L. Landrieu. Weakly supervised segmentation-aided classification of urban scenes from 3d lidar point clouds. *ISPRS - International Archives of the Photogrammetry, Remote Sensing and Spatial Information Sciences*, XLII-1/W1:151–157, 2017.

Jan Hackenberg, Heinrich Spiecker, Kim Calders, Mathias Disney, and Pasi Raumonen. Simpletree—an efficient open source tool to build tree models from tls clouds. *Forests*, 6(11):4245–4294, 2015a.

Jan Hackenberg, Marc Wassenberg, Heinrich Spiecker, and Dongjing Sun. Non destructive method for biomass prediction combining tls derived tree volume and wood density. *Forests*, 6(4):1274–1300, 2015b.

Franck Hétroy-Wheeler, Eric Casella, and Dobrina Boltcheva. Segmentation of tree seedling point clouds into elementary units. *International Journal of Remote Sensing*, 37(13):2881–2907, 2016.

Sanna Kaasalainen, Anssi Krooks, Antero Kukko, and Harri Kaartinen. Radiometric calibration of terrestrial laser scanners with external reference targets. *Remote Sensing*, 1(3):144–158, 2009.

Sanna Kaasalainen, Anssi Krooks, Jari Liski, Pasi Raumonen, Harri Kaartinen, Mikko Kaasalainen, Eetu Puttonen, Kati Anttila, and Raisa Mäkipää. Change detection of tree biomass with terrestrial laser scanning and quantitative structure modelling. *Remote Sensing*, 6(5):3906–3922, 2014.

Klaas Klasing, Dirk Wollherr, and Martin Buss. A clustering method for efficient segmentation of 3d laser data. In *2008 IEEE International Conference on Robotics and Automation*, pages 4043–4048. IEEE, 2008.

S. M. Krishna Moorthy, K. Calders, M. B. Vicari, and H. Verbeeck. Improved supervised learning-based approach for leaf and wood classification from lidar point clouds of forests. *IEEE Transactions on Geoscience and Remote Sensing*, pages 1–14, 2019. ISSN 1558-0644. doi: 10.1109/TGRS.2019.2947198.

Loïc Landrieu, Hugo Raguet, Bruno Vallet, Clément Mallet, and Martin Weinmann. A structured regularization framework for spatially smoothing semantic labelings of 3d point clouds. *ISPRS Journal of Photogrammetry and Remote Sensing*, 132:102–118, 2017.

Alvaro Lau, Lisa Patrick Bentley, Christopher Martius, Alexander Shenkin, Harm Bartholomeus, Pasi Raumonen, Yadvinder Malhi, Tobias Jackson, and Martin Herold. Quantifying branch architecture of tropical trees using terrestrial lidar and 3d modelling. *Trees*, 32(5):1219–1231, 2018.

Alvaro Lau, Kim Calders, Harm Bartholomeus, Christopher Martius, Pasi Raumonen, Martin Herold, Matheus Vicari, Hansrajie Sukhdeo, Jeremy Singh, and Rosa C Goodman. Tree biomass equations from terrestrial lidar: A case study in guyana. *Forests*, 10(6):527, 2019.

Nan Li, Chun Liu, and Norbert Pfeifer. Improving lidar classification accuracy by contextual label smoothing in post-processing. *ISPRS journal of photogrammetry and remote sensing*, 148:13–31, 2019.

Shihua Li, Leiyu Dai, Hongshu Wang, Yong Wang, Ze He, and Sen Lin. Estimating leaf area density of individual trees using the point cloud segmentation of terrestrial lidar data and a voxel-based model. *Remote Sensing*, 9(11):1202, 2017.

Xinlian Liang, Ville Kankare, Juha Hyyppä, Yunsheng Wang, Antero Kukko, Henrik Haggrén, Xiaowei Yu, Harri Kaartinen, Anttoni Jaakkola, Fengying Guan, et al. Terrestrial laser scanning in forest inventories. *ISPRS Journal of Photogrammetry and Remote Sensing*, 115:63–77, 2016.

Lixia Ma, Guang Zheng, Jan UH Eitel, L Monika Moskal, Wei He, and Huabing Huang. Improved salient feature-based approach for automatically separating photosynthetic and nonphotosynthetic components within terrestrial lidar point cloud data of forest canopies. *IEEE Transactions on Geoscience and Remote Sensing*, 54(2):679–696, 2015.

Åkerblom Markku, Pasi Raumonen, Mikko Kaasalainen, and Eric Casella. Analysis of geometric primitives in quantitative structure models of tree stems. *Remote Sensing*, 7 (4):4581–4603, 2015.

S Momo, Takoudjou, P Ploton, B Sonké, J Hackenberg, S Griffon, F de, Coligny, NG Kamdem, M Libalah, GI Mofack, G Le, Moguédec, R Pélissier, and N Barbier. Data from: Using terrestrial laser scanning data to estimate large tropical trees biomass and calibrate allometric models: a comparison with traditional destructive approach, 2017. URL https://doi.org/10.5061/dryad.10hq7.

Stéphane Momo Takoudjou, Pierre Ploton, Bonaventure Sonké, Jan Hackenberg, Sébastien Griffon, François De Coligny, Narcisse Guy Kamdem, Moses Libalah, Gislain II Mofack, Gilles Le Moguédec, et al. Using terrestrial laser scanning data to estimate large tropical trees biomass and calibrate allometric models: A comparison with traditional destructive approach. *Methods in Ecology and Evolution*, 9(4):905–916, 2018.

Glenn J Newnham, John D Armston, Kim Calders, Mathias I Disney, Jenny L Lovell, Crystal B Schaaf, Alan H Strahler, and F Mark Danson. Terrestrial laser scanning for plot-scale forest measurement. *Current Forestry Reports*, 1(4):239–251, 2015.

Ian Paynter, Daniel Genest, Edward Saenz, Francesco Peri, Zhan Li, Alan Strahler, and Crystal Schaaf. Quality assessment of terrestrial laser scanner ecosystem observations using pulse trajectories. *IEEE Transactions on Geoscience and Remote Sensing*, 56 (11):6324–6333, 2018.

Norbert Pfeifer, Ben Gorte, Daniel Winterhalder, et al. Automatic reconstruction of single trees from terrestrial laser scanner data. In *Proceedings of 20th ISPRS Congress*, volume 35, pages 114–119. ISPRS Istanbul, 2004.

Norbert Pfeifer, Bernhard Höfle, Christian Briese, Martin Rutzinger, and Alexander Haring. Analysis of the backscattered energy in terrestrial laser scanning data. *Int. Arch. Photogramm. Remote Sens. Spat. Inf. Sci*, 37:1045–1052, 2008.

P. Raumonen, E. Casella, K. Calders, S. Murphy, M. Åkerblom, and M. Kaasalainen. Massive-scale tree modelling from tls data. *ISPRS Annals of Photogrammetry, Remote Sensing and Spatial Information Sciences*, II-3/W4:189–196, 2015.

Pasi Raumonen and Tanja Tarvainen. Segmentation of vessel structures from photoacoustic images with reliability assessment. *Biomedical optics express*, 9(7):2887–2904, 2018.

Pasi Raumonen, Mikko Kaasalainen, Markku Åkerblom, Sanna Kaasalainen, Harri Kaartinen, Mikko Vastaranta, Markus Holopainen, Mathias Disney, and Philip Lewis. Fast automatic precision tree models from terrestrial laser scanner data. *Remote Sensing*, 5(2):491–520, 2013.

Johannes Strom, Andrew Richardson, and Edwin Olson. Graph-based segmentation for colored 3d laser point clouds. In *2010 IEEE/RSJ International Conference on Intelligent Robots and Systems*, pages 2131–2136. IEEE, 2010.

Shengli Tao, Qinghua Guo, Shiwu Xu, Yanjun Su, Yumei Li, and Fangfang Wu. A geometric method for wood-leaf separation using terrestrial and simulated lidar data. *Photogrammetric Engineering & Remote Sensing*, 81(10):767–776, 2015.

Jan Trochta, Martin Krůček, Tomáš Vrška, and Kamil Král. 3d forest: An application for descriptions of three-dimensional forest structures using terrestrial lidar. *PLOS ONE*, 12(5):1–17, 05 2017.

Matheus B Vicari, Mathias Disney, Phil Wilkes, Andrew Burt, Kim Calders, and William Woodgate. Leaf and wood classification framework for terrestrial lidar point clouds. *Methods in Ecology and Evolution*, 10(5):680–694, 2019a.

Matheus Boni Vicari. *On leaf and wood separation from Terrestrial LiDAR data*. PhD thesis, UCL (University College London), 2019.

Matheus Boni Vicari, Jan Pisek, and Mathias Disney. New estimates of leaf angle distribution from terrestrial lidar: Comparison with measured and modelled estimates from nine broadleaf tree species. *Agricultural and forest meteorology*, 264:322–333, 2019b.

D. Wang, M. Hollaus, and N. Pfeifer. Feasibility of machine learning methods for separating wood and leaf points from terrestrial laser scanning data. *ISPRS Annals of Photogrammetry, Remote Sensing and Spatial Information Sciences*, IV-2/W4:157–164, 2017.

Di Wang, Markus Hollaus, Eetu Puttonen, and Norbert Pfeifer. Automatic and self-adaptive stem reconstruction in landslide-affected forests. *Remote Sensing*, 8(12):974, 2016.

Di Wang, Jasmin Brunner, Zhenyu Ma, Hao Lu, Markus Hollaus, Yong Pang, and Norbert Pfeifer. Separating tree photosynthetic and non-photosynthetic components from point cloud data using dynamic segment merging. *Forests*, 9(5):252, 2018.

Phil Wilkes, Alvaro Lau, Mathias Disney, Kim Calders, Andrew Burt, Jose Gonzalez de Tanago, Harm Bartholomeus, Benjamin Brede, and Martin Herold. Data acquisition considerations for terrestrial laser scanning of forest plots. *Remote Sensing of Environment*, 196:140–153, 2017.

Ting Yun, Feng An, Weizheng Li, Yuan Sun, Lin Cao, and Lianfeng Xue. A novel approach for retrieving tree leaf area from ground-based lidar. *Remote Sensing*, 8(11): 942, 2016.

Junjie Zhou, Hongqiang Wei, Guiyun Zhou, and Lihui Song. Separating leaf and wood points in terrestrial laser scanning data using multiple optimal scales. *Sensors*, 19(8), 2019.

Xi Zhu, Andrew K Skidmore, Roshanak Darvishzadeh, K Olaf Niemann, Jing Liu, Yifang Shi, and Tiejun Wang. Foliar and woody materials discriminated using terrestrial lidar in a mixed natural forest. *International journal of applied earth observation and geoinformation*, 64:43–50, 2018.

Markku Åkerblom. Inversetampere/treeqsm: Initial release, August 2017. URL https://doi.org/10.5281/zenodo.844626.